JOURNAL OF GUIDANCE, CONTROL, AND DYNAMICS
Vol. 23, No. 3, May–June 2000

Perspective Predictor/Flight-Path Display with Minimum Pilot Compensation

Gottfried Sachs*
Technical University of Munich, 85747 Garching, Germany

Prediction can substantially enhance the novel guidance and control capabilities of perspective flight-path displays. A position predictor based on geometry/kinematics relations is considered, and an extension based on manual control theory issues is introduced. Pilot-centered requirements for compensatory control of the predictor–aircraft system are considered. It is shown which are the effects on pilot–predictor–aircraft system crossover, system stability, response quality, and system bandwidth. A solution for a predictor with minimum pilot compensation is presented. Furthermore, it is shown that the flight-path predictor is also an efficient means for controlling the current state of the aircraft. The conceptual and theoretical predictor considerations are verified with pilot-in-the-loop simulation experiments.

Nomenclature

e = error
g = acceleration due to gravity
K = gain
L_{δ_a} = roll moment due to roll control input
s = Laplace operator
T = time constant
$Y(s)$ = transfer function
y = lateral coordinate
Δ = denoting a perturbation, for example, Δy
δ_a = roll control
ζ = damping ratio
τ_e = effective time delay
ϕ = roll angle
χ = azimuth angle
ω = frequency

Introduction

PERSPECTIVE flight-path displays with a predictor are an innovative instrumentation type because they provide the pilot with three-dimensional information of the current and the future aircraft states and the future command flight-path. Thus, they offer a fundamental improvement over current cockpit instrumentation, which presents two-dimensional information of current aircraft position and actual flight condition. With conventional instrumentation, the pilot mentally reconstructs the spatial and temporal situation of the aircraft from planar displays. By contrast, a perspective flight-path display presents information in a spatial format and, thus, provides a basic advancement for the cockpit instrumentation. A further improvement is possible by presenting an object such that the emergent features can be directly perceived so that the pilot does not have to decompose the object into features. Rather, the manner in which the flight-path is presented allows holistic perception. A recent paper provides guidelines for designing the parameters of a perspective flight-path display that takes the specific human capabilities in the areas of perception, cognition, and control into account.[1]

Recent research, including simulation experiments and flight tests, shows that substantial improvements in aircraft guidance and control can be achieved with pictorial perspective flight-path displays with a predictive capability.[1–13] The flight test verification includes the first landing of an aircraft with a pictorial display presenting three-dimensional guidance information (synthetic vision) as the only visual information for the pilot.[11,12]

Received 11 March 1999; revision received 30 September 1999; accepted for publication 3 October, 1999.

*Director, Institute of Flight Mechanics and Flight Control, Boltzmannstrasse 15. Fellow AIAA.

The predictor symbol in a tunnel display was treated, and its advantage was demonstrated through theoretical as well as experimental investigations. In Ref. 3, it is shown that a tunnel display with a predictor outperforms conventional-type displays. The advantage of the predictor symbol is demonstrated through pilot simulation and in an exploratory flight test. A detailed investigation of the predictor symbol is presented in Ref. 4, which shows that more complex predictive information indicating future position and attitude has only a marginal advantage over more basic predictive information. In Ref. 5, different predictor laws related to circular and full-order models are applied, and a pilot–vehicle stability analysis is undertaken with the assumption of a pure-gain pilot model. References 6 and 7 are concerned with improvements in the display layout, yielding an algorithm for generating well-matched trajectory shapes and improved predictor guidance information, with a circular predictor model applied. In the context of providing predictive information, Ref. 14, which includes both pilot–vehicle analysis and pilot simulation results is of interest because it deals with a predictor symbol, the dynamics of which are designed to yield transfer characteristics that are desirable from the standpoint of manual control response and performance.

In summary, the predictor models hitherto used in perspective flight-path displays are based on geometry/kinematics relations because their intent is to predict the future aircraft position and the continuation of the flight path. Their effectiveness was primarily demonstrated through experimental investigations, supplemented by stability analyses using an assumed pure-gain pilot model.

The purpose of this paper is basically twofold: First, the predictor concept based on geometry/kinematics relations will be assessed by means of manual control theory. Thus, possible deficiencies that may exist from the standpoint of manual control theory can be identified. Furthermore, it will be shown that manual control theory provides explanations for predictor characteristics effects, like the significant effect of the prediction time and its optimal selection. Second, a new predictor concept is introduced that is based on manual control issues (appropriately combined with geometry/kinematics considerations). The proposed approach uses manual control theory as a design tool for perspective predictor/flight-path displays. It will be shown that this predictor concept yields a predictor–aircraft system requiring minimum pilot compensation and, thus, can substantially contribute to the improvement of manual control performance.

Novel Guidance and Control Capabilities with Perspective Predictor/Flight-Path Display

Perspective flight-path displays with a predictor provide novel guidance information for the pilot. This is illustrated in Fig. 1, which shows a perspective flight-path display presenting the command flight path in three-dimensional form (tunnel) and a predictive element (predictor) as well as other, integrated guidance elements.

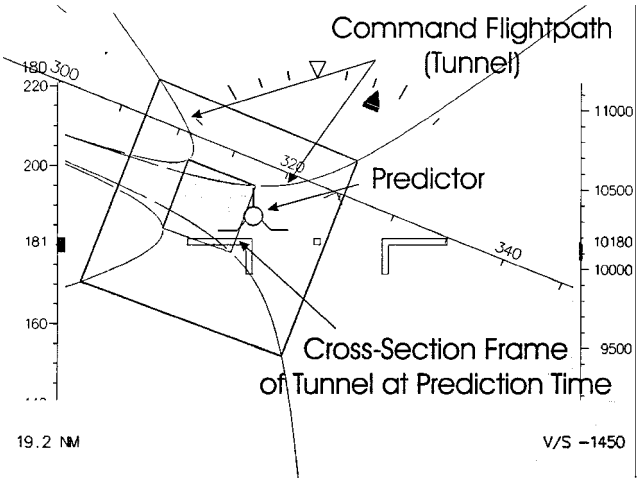

Fig. 1 Predictive flight-path display with three-dimensional flight-path presentation.

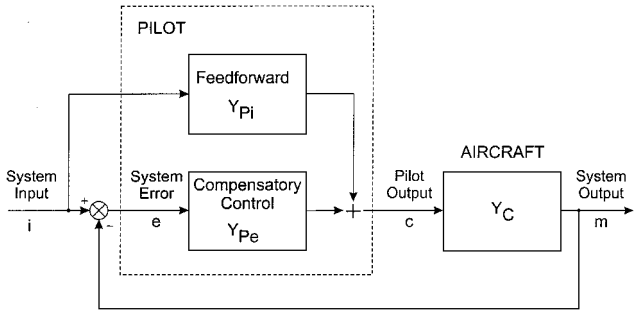

Fig. 2 Model for dual-mode pilot–aircraft system.

A more detailed inspection of Fig. 1 shows that the predictor indicates the future position of the aircraft at a specified time ahead (prediction time). The predictor is referenced to the command flight path with the use of a specially marked cross-section frame of the command flight path. This cross-section frame indicates the command position at the prediction time ahead. A deviation of the predictor from the center of the cross-section frame of the command flight path provides the pilot with a precise indication of the position error at the prediction time ahead.

The three-dimensional visual information displayed to the pilot enables him to apply novel control modes when compared with cockpit instrumentation presenting two-dimensional information of the current aircraft state. Figure 2 shows a simplified model for describing general pathways of the human controller operating on visually sensed inputs and exerting manual control outputs. Different control modes described in the following sections are possible.

Compensatory Control

The compensatory control mode is a closed-loop control for regulation tasks. The pilot, who primarily acts in response to errors or vehicle output quantities Y_{Pe}, can exert continuous control over the aircraft for minimizing system errors in the presence of command and/or disturbance inputs. Compensatory control is applied when system errors are the only source of information available.

For perspective flight-path displays with predictive capability, the predictor shows the position of the aircraft at the prediction time ahead. It indicates, with reference to the command flight-path, the (future) position error. From a control point of view, the predictive capability of a perspective flight-path display is, therefore, an issue primarily related to compensatory control.

Pursuit/Preview Control

When command information and preview are available, the pilot can use this preview to structure a control feedforward Y_{Pi} (Fig. 2). The open-loop feedforward element permits the pilot to anticipate the future flight-path. The pursuit/preview control mode often appears in company with compensatory operations as a dual-mode control forming a combination open-loop, closed-loop control action. In this form, the control is initiated and can be largely accomplished by the feedforward control action and may be finished with compensatory actions for error reduction.

With perspective flight-path displays, command information and preview are available with the three-dimensional future trajectory presented to the pilot as the command flight-path. From a control point of view, the command flight-path presentation is, therefore, an issue related to pursuit/preview control and, in combination with the predictor, to compensatory control.

Summing up the modes possible with predictive flight-path displays, the control is either compensatory, pursuit/preview, or dual mode. In dual-mode phases, the feedforward element operates on inputs provided from the predictive flight-path display presenting information about the current and future flight conditions, and the closed-loop control element is a fine adjustment component for reducing errors.

The focus of the paper is on compensatory control related to predictive flight-path displays as an important issue of this novel display type. This is because the predictive capability of a perspective flight-path display basically is a compensatory control issue. Although predictor control originally concerns an error state in the future at the prediction time ahead, it will be shown that the predictor-related compensatory control is also very efficient for minimizing the error of the current state.

Pilot-Centered Requirements for Compensatory Predictor Control

The compensatory control problem in mind, where the pilot continuously tries to minimize an error in a closed-loop manner, is illustrated in Fig. 3, which shows a model for the pilot–predictor–aircraft system. There are pilot-centered requirements that result from the presence of the human operator in the control loop. They concern the effort required by the pilot for performing the control task. The objective is to achieve an overall predictive system requiring minimum pilot compensation.

The following general form of the pilot describing function model holds for aircraft applications,[15,16] including the compensatory control problem in mind:

$$Y_P(s) = K_P[(T_L s + 1)/(T_I s + 1)]e^{-\tau_e s} \tag{1}$$

where K_P is a gain, T_L and T_I are lead and lag time constants, and τ_e is an effective time delay.

The pilot can set the parameters of Eq. (1) for a satisfactory behavior of the controlled element (predictor–aircraft system) by appropriate equalization selection and adjustment. For the compensatory control problem, equalization for minimum pilot effort and best performance is a primary goal. The corresponding selection of the parameters of Eq. (1) is a basic issue for the synthesis of the predictor.

Manual control theory and related experimental verification show that the crossover model can be applied to pilot–aircraft systems for a great variety of controlled elements and input commands.[15,16] For the controlled element in mind, the predictor–aircraft system $Y_{PR}Y_C$, the crossover model form yields

$$Y_P Y_{PR} Y_C = \omega_C e^{-\tau_e s} \Big| \; s \tag{2}$$

This relation holds for the region centered around the crossover frequency ω_C.

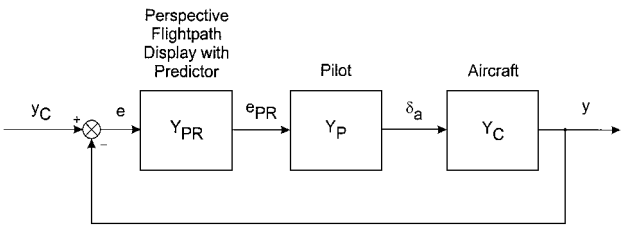

Fig. 3 Pilot–predictor–aircraft model for compensatory control.

The pilot can adapt his characteristics described by $Y_P(s)$ to compensate for a variety of dynamics of the controlled aircraft–predictor element, $Y_C(s)$ and $Y_{PR}(s)$, such that the crossover model form Eq. (2) holds. This concerns possible dynamic deficiencies for which the pilot may develop low-frequency lead or adjust his gain. When a low-frequency lead is required, the associated cost is increased pilot time delay, degraded system performance, and a decrement in pilot ratings.

For achieving the best results in terms of performance and workload, a design requirement is that the predictive system should be constructed to require no low-frequency lead equalization for the pilot and to permit pilot loop closure over a wide range of gains.[15] This pilot-centered requirement can be met when the equalizations and gains are selected so that the effective transfer characteristic of the controlled element, the predictor–aircraft system $Y_{PR}(s)Y_C(s)$, approximates either a pure gain or a pure integration over an adequately broad region centered around the pilot–predictor–aircraft crossover, that is, for pure gain,

$$Y_{PR}(s)Y_C(s) = K \tag{3a}$$

and for pure integration,

$$Y_{PR}(s)Y_C(s) = K/s \tag{3b}$$

The pure gain case, however, may be not an appropriate solution. This is because the dynamics of the aircraft between aileron and predictor position cannot be made a gain without introducing characteristics that may be undesirable or even unrealistic. It leads to a higher-order predictor that requires roll rate feedback with a high gain. This can yield the violation of a requirement for face validity, according to which status information presented by the predictor in the perspective flight-path display should correspond to the actual situation.

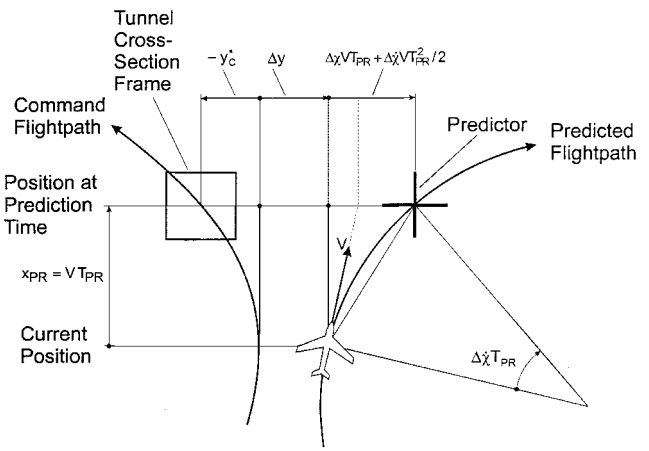

Fig. 4 Lateral displacement of basic predictor with circular flight-path continuation.

Therefore, the integrator characteristic Eq. (3b) is selected, which is nearly as good as a pure gain with regard to pilot response and performance. It is considered to have distinct advantages over the pure gain case as a basis for the design of the flight-path predictor.

Equation (3b) describes desired dynamic characteristics of the predictor–aircraft system as the controlled element. This can be used as key requirement for designing the predictor to achieve appropriate dynamic characteristics of the closed-loop pilot–predictor–aircraft system.

For a predictor–aircraft system as described by Eq. (3b), it follows from Eq. (1) that the pilot behavior can be modeled as (with $\omega_C = KK_P$)

$$Y_P(s) = K_P e^{-\tau_e s} \tag{4}$$

Further dynamic requirements that are significant for the closed-loop characteristics concern system stability, response quality, and system bandwidth. The closed-loop system should have an adequate stability level, including good system damping. Response quality refers to certain predictor/flight-path response aspects that are concerned with subjective pilot opinion of the system. It includes predictor response characteristics (consistency of predictor signal with vehicle or control motions) and vehicle motion response characteristics (modal interaction/separation). Good command following and disturbance regulation requires an adequate bandwidth of the closed-loop system.

Summing up the foregoing considerations, the following dynamic requirements are of concern: 1) predictor–aircraft transfer characteristics in the frequency region of pilot–predictor–aircraft system crossover, 2) system stability, 3) response quality, and 4) system bandwidth.

This paper emphasizes lateral predictor control and related system characteristics, but the procedure and considerations can also be applied for the longitudinal motion.

Basic Predictor (Circular Flight-Path Continuation)

The purpose of flight-path prediction is to provide the pilot with an indication of the future flight path. Prediction is based on an estimated flight-path continuation for which different models of various order are applied. A second-order model yielding a circular continuation of the flight path represents a promising predictor concept.[1,3–8,10] From the relations in Fig. 4, which shows geometry and kinematics for circular flight-path continuation, it follows that the deviation of the predicted position from the command flight path at the prediction time T_{PR} ahead may be expressed as

$$\Delta y_{PR} = \Delta y - y_C^* + \Delta\chi VT_{PR} + \Delta\dot{\chi}VT_{PR}^2 \Big| 2 \tag{5}$$

The block diagram presented in Fig. 5 shows how the predicted position displacement Δy_{PR} can be determined with relations of the current aircraft state. With the use of these relations, the transfer characteristics between the position error e_{PR} presented by the

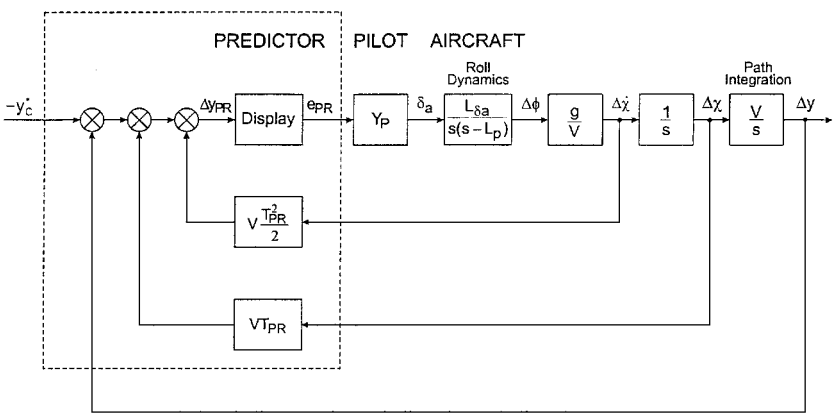

Fig. 5 Block diagram for basic predictor with circular flight-path continuation.

predictor symbol and the roll angle $\Delta\phi$ may be expressed after Laplace transformation as

$$Y_{PR} = \frac{e_{PR}(s)}{\Delta\phi(s)} = K_{PR}g\frac{(T_{PR}^2/2)s^2 + T_{PR}s + 1}{s^2} \tag{6}$$

where

$$e_{PR}(s) = K_{PR}\Delta y_{PR}(s) \tag{7}$$

The transfer function Eq. (6) describes the dynamic behavior of the predictor. There are two factors, T_{PR} and K_{PR}, that can be selected for best equalization for the controlled aircraft–predictor element.

The dynamics of the aircraft can be described with the roll mode characterized by its time constant T_R because it can be considered to be the dominant root of the vehicle for the frequency region of concern. Accordingly,

$$Y_C = \frac{\Delta\phi(s)}{\delta_a(s)} = \frac{L_{\delta_a}}{s(s + 1/T_R)} \tag{8}$$

Combining Eqs. (6) and (8) yields the following expression for the open-loop predictor–aircraft transfer function (effective predictor to control response, without pilot):

$$Y_{PR}Y_C = \frac{e_{PR}(s)}{\delta_a(s)} = K_{PR}gL_{\delta_a}\frac{T_{PR}^2}{2}\frac{s^2 + (2/T_{PR})s + 2/T_{PR}^2}{s^3(s + 1/T_R)} \tag{9}$$

The zeros of the numerator, which may be rewritten as

$$s^2 + 2\zeta_{PR}\omega_{PR}s + \omega_{PR}^2 = s^2 + (2/T_{PR})s + 2/T_{PR}^2 \tag{10}$$

are given by

$$\omega_{PR} = \sqrt{2}/T_{PR}, \qquad \zeta_{PR} = 1/\sqrt{2} \tag{11}$$

Compensatory Control (Basic Predictor)

The predictor–aircraft transfer characteristics that are of concern for compensatory control are illustrated in Fig. 6, which presents a system survey (with data of the aircraft used in the simulation experiments described in a subsequent section). An asymptotic Bode plot is used to address this issue. As a main result, Fig. 6 shows, in accordance with Eq. (9), that there is a K/s characteristic in the frequency region between ω_{PR} and $1/T_R$. This is the frequency region where pilot–system crossover is possible. From $\omega_{PR} = \sqrt{2}/T_{PR}$ and from Eq. (9), it follows as a general characteristic that the K/s frequency region is primarily determined by T_{PR} and T_R. The length of the K/s frequency region decreases with a decrease of the difference between T_{PR} and T_R and vice versa. This is a basic result according to which T_{PR} may be selected with reference to the value of T_R to assure a K/s frequency region large enough. If, for example, a T_{PR} value is selected close to T_R, the resulting K/s frequency region may be too small or not even achieved. In that case, the pilot would have to develop a lead characteristic that would incur a cost as described earlier.

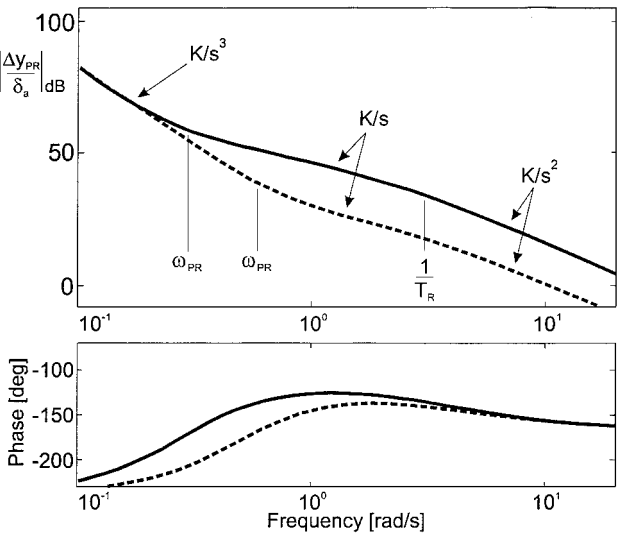

Fig. 6 Bode plot for predictor–aircraft system (basic predictor with circular flight-path prediction): ——, T_{PR} = 5.0 s, and – – –, T_{PR} = 2.5 s.

With regard to the effect of aircraft dynamics, the roll mode time constant T_R is of primary concern for the K/s frequency region. The roll mode time constant is a primary flying qualities metric for which an acceptable range is specified, including appropriate limits.[17,18] This range and its limiting values, respectively, can be used to provide an estimation for the prediction time T_{PR}. A range of 0.3–1.0 s may be considered as realistic for T_R when taking related flying qualities requirements into account.[17,18] If the objective is to achieve a decade of K/s frequency region, a range of about 5–10 s may be a reasonable choice for T_{PR} when also taking stability and bandwidth issues, dealt with in a subsequent section, into account.

There is a further effect of the prediction time T_{PR} for compensatory control, in addition to the effect on the length of the K/s frequency region. It concerns the pilot gain required for crossover in the K/s frequency region. If T_{PR} is decreased, the pilot gain for crossover has to be increased (and vice versa). This is because a T_{PR} decrease leads to a prolongation of the K/s^3 frequency region until the increased ω_{PR} frequency value ($\omega_{PR} = \sqrt{2}/T_{PR}$) is reached where the K/s region begins (Fig. 6). The prolongation of the K/s^3 frequency region yields a downward shift of the amplitude values in the K/s frequency region so that an increase of pilot gain for loop closure is required.

This result can be confirmed by considering the condition at pilot–system crossover. Here, the following relation holds:

$$|Y_P Y_{PR} Y_C|_{s=i\omega_C} = \left| K_P K_C^* e^{-\tau_e s}\frac{s^2 + 2\zeta_{PR}\omega_{PR}s + \omega_{PR}^2}{s^3(T_R s + 1)}\right|_{s=i\omega_C} = 1 \tag{12}$$

where $K_C^* = -(g/2)K_{PR}L_{\delta_a}T_{PR}^2T_R$. For $\omega_C \gg \omega_{PR}$, it follows from Eq. (12) that

$$|K_P| \approx (1/K_C^*)(\omega_C/|iT_R\omega_C + 1|) \tag{13}$$

Manual control theory shows that system crossover frequency ω_C is invariant with controlled element gain.[15] This means that for the problem in mind, ω_C can be considered constant as regards a change of T_{PR} (provided that the K/s frequency region remains large enough). Thus, it follows from Eq. (13) that

$$|K_P| \propto 1/T_{PR}^2 \tag{14}$$

As a result, there is an increase in pilot gain K_P with a decrease of T_{PR}.

Stability, Response Quality, and Bandwidth (Basic Predictor)

The stability characteristics of the closed-loop system can be evaluated with the root locus technique yielding results of rather general nature. Figure 7 presents the root locus of a pilot closure for the aircraft used in the simulation experiments, where the pilot model,

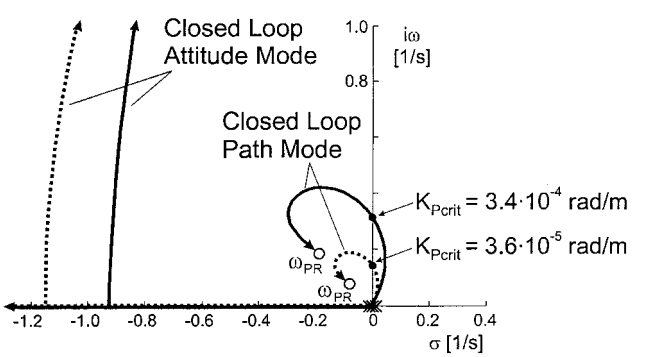

Fig. 7 Root locus of closed-loop system with basic predictor [T_I = 0.3 s, pilot model Eq. (4) with τ_e = 0.25 s, K_{PR} = 1.0]: ——, T_{PR} = 5.0 s, and - - - -, T_{PR} = 10.0 s.

Eq. (4), valid for the K/s characteristic, is applied. Figure 7 shows that there are basically two root locus branches. Correspondingly, there are two closed-loop modes from which the lower frequency mode is primarily related to path control whereas the other one concerns attitude. Furthermore, Fig. 7 shows that system stability is achieved above a certain pilot gain $K_{P_{\text{crit}}}$. Figure 7 also indicates that $K_{P_{\text{crit}}}$ is increased if a smaller T_{PR} value is selected.

Response quality is another issue. The root locus presented in Fig. 7 shows that there are two modes of motion of which the one at low frequency may be identified as a path mode and the other as an attitude mode. The path and attitude modes that show rapid and adequately damped response characteristics are well separated in frequency, and there appears to be no coupling problem. From the root locus characteristics it further follows that pilot loop closure does not drive the system modes into near proximity. Predictor response quality refers to correspondence between the signal presented by the predictor position in the perspective flight-path display and the vehicle or control motions. The predictor position in relation to the flight-path corresponds to the predicted displacement of the position of the aircraft so that there is consistency with trajectory deviation and aircraft heading.

A further issue is closed-loop system bandwidth. Good command following and disturbance regulation require a large enough bandwidth. From the root locus presentation of Fig. 7, it follows that the frequency ω_{PR} of the numerator zeros of the predictor transfer function, Eqs. (9) and (11), is significant for the maximum achievable closed-loop system bandwidth. Because $\omega_{PR} = \sqrt{2}/T_{PR}$, the bandwidth is increased when a smaller T_{PR} is selected. As a consequence, bandwidth is in conflict with predictor–aircraft transfer characteristics and stability so that the selection of T_{PR} involves a tradeoff between them. However, a more detailed investigation shows that some improvement is possible because there is a root locus part where the closed-loop system frequencies are larger than ω_{PR} (Fig. 7).

Predictor Extension: Roll Rate Feedback

An extension of the predictor concept is introduced that concerns the upper part of the K/s frequency region when $1/T_R$ is approached. From the Bode plot in Fig. 6, it follows that there is a K/s^2 characteristic for frequencies greater than $1/T_R$. For this frequency region, there may be a need for the pilot to develop a lead to cancel the effect of $1/T_R$ for achieving a K/s characteristic. Such a need is more pronounced with aircraft having a large roll time constant T_R. If the addressed effect is significant enough, the crossover frequency is reduced and the effective time delay of the pilot is increased.[15,16] As a consequence, a deterioration in performance results. A pilot lead can be avoided with a predictor extension by introducing roll rate feedback for the predictor control law and selecting an appropriate gain for this pathway.

With roll rate feedback $K_{\dot\phi}\dot\phi$, the displacement of the predicted position from the command flight-path may be expressed as

$$\Delta y_{PR} = \Delta y - y_C^* + \Delta\chi VT_{PR} + \Delta\dot\chi VT_{PR}^2 \left| \; 2 + K_{\dot\phi}\dot\phi \right. \tag{15}$$

Accordingly, the predictor dynamics read

$$Y_{PR} = \frac{e_{PR}(s)}{\Delta\phi(s)} = K_{PR} g \frac{(K_{\dot\phi}/g)s^3 + \left(T_{PR}^2 \left| \; 2\right.\right)s^2 + T_{PR}s + 1}{s^2} \tag{16}$$

With Eq. (8), the following relation for the predictor–aircraft transfer function results:

$$Y_{PR}Y_C = \frac{e_{PR}(s)}{\delta_a(s)} = K_{PR}K_{\dot\phi}L_{\delta_a} \times \frac{s^3 + \left[gT_{PR}^2 \left| \; (2K_{\dot\phi})\right.\right]s^2 + (gT_{PR}/K_{\dot\phi})s + g/K_{\dot\phi}}{s^3(s + 1/T_R)} \tag{17}$$

The purpose of roll rate feedback is to introduce an additional open-loop zero s_{PR} and place it the close to roll mode root $-1/T_R$ to achieve the cancellation effect described. Assuming $1/T_R \gg \omega_{PR}$, the following relation between the zero introduced by roll rate feedback s_{PR} and the two other path related zeros ω_{PR} and ζ_{PR} holds:

$$|s_{PR}| \gg \omega_{PR} \tag{18}$$

Based on this relation, a factorization of the transfer function numerator Eq. (17) that may be rewritten as

$$(s - s_{PR})\left(s^2 + 2\zeta_{PR}\omega_{PR}s + \omega_{PR}^2\right) = s^3 + \left[gT_{PR}^2 \left| \; (2K_{\dot\phi})\right.\right]s^2 + (gT_{PR}/K_{\dot\phi})s + g/K_{\dot\phi}$$

yields the following approximate solutions

$$s_{PR} \approx -gT_{PR}^2 \left| \; (2K_{\dot\phi}), \qquad \omega_{PR} \approx \omega_{PR_0}, \qquad \zeta_{PR} \approx \zeta_{PR_0} \right. \tag{19}$$

where $\omega_{PR_0} = \sqrt{2}/T_{PR}$ and $\zeta_{PR_0} = 1/\sqrt{2}$ denote the circular predictor case, Eqs. (10) and (11). Equation (19) shows that a desired value of s_{PR} can be achieved by selecting an appropriate roll rate feedback gain $K_{\dot\phi}$ whereas ω_{PR} and ζ_{PR} are approximately independent of $K_{\dot\phi}$.

For compensatory control, the main effect of roll rate feedback concerns cancellation of the roll mode root $-1/T_R$. For this purpose ($s_{PR} \approx -1/T_R$), the roll rate feedback gain may be selected as

$$K_{\dot\phi} \approx (g/2)T_R T_{PR}^2 \tag{20}$$

With this gain selection, the following simple form of the predictor–aircraft transfer function results from Eq. (17):

$$Y_{PR}Y_C \approx K_C^* \frac{s^2 + 2\zeta_{PR}\omega_{PR}s + \omega_{PR}^2}{s^3} \tag{21}$$

This relation shows that the K/s frequency region extends to values higher than $1/T_R$. Thus, the controlled predictor–aircraft element is K/s-like for all practically interesting frequencies in the high-frequency region. This is shown in Fig. 8, which presents the effect of roll rate feedback on frequency response characteristics, with a gain selection according to Eq. (20). From Fig. 8, it is evident that the effect of roll rate feedback is especially advantageous for aircraft with large roll mode time constant T_R.

For the condition at pilot–system crossover for the predictor with roll rate feedback, the following relation holds:

$$|Y_P Y_{PR} Y_C|_{s=i\omega_C} \approx \left| K_P K_C^* e^{-\tau_e s} \frac{s^2 + 2\zeta_{PR}\omega_{PR}s + \omega_{PR}^2}{s^3} \right|_{s=i\omega_C} \approx 1 \tag{22}$$

For $\omega_C \gg \omega_{PR}$, it follows from Eq. (22) that

$$|K_P| \approx \omega_C \left| \; K_C^* \right. \tag{23}$$

The pilot–system crossover frequency ω_c can be considered constant and, thus, is invariant with $K_C^* = -(g/2)K_{PR}L_{\delta_a}T_{PR}^2T_R$. This

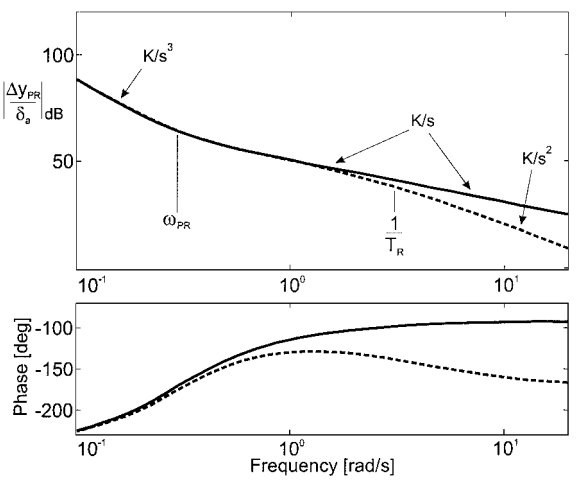

Fig. 8 Effect of roll rate feedback on frequency response characteristics of predictor–aircraft system: ——, roll rate feedback, and – – –, no roll rate feedback.

result implies that ω_C is invariant with the open-loop roll time constant T_R. Furthermore, there is an increase of K_P with a decrease of T_{PR} (as it holds for the basic predictor):

$$|K_P| \propto 1/T_{PR}^2 \tag{24}$$

The predictor extension introduced in this paper is a new concept element for the design of predictors. This is because it is based on control systems considerations (appropriately combined with geometry/kinematics considerations). The primary objective of the new concept element is to improve the characteristics of the closed-loop pilot–predictor–aircraft system by applying appropriate control techniques means.

Stability, Response Quality, and Bandwidth (Predictor Extension)

The stability characteristics of the closed-loop system with the predictor extension (using aircraft data of the simulation experiments) are graphically illustrated in Fig. 9. The low-frequency roots denote the path mode that is similar to the basic predictor case. Thus, the positive characteristics of the closed-loop path mode existing with the basic predictor are retained. The high-frequency root concerns the attitude mode. The attitude mode is now an aperiodic mode of motion instead of an oscillatory one (as in the basic predictor case). This is a difference between the two predictor types. Furthermore, there is an improvement of system stability due to the increase in the phase at frequencies around $1/T_R$ and above (Fig. 8). This stability improvement is especially advantageous for aircraft with large roll mode time constant T_R. There is a fourth high-frequency root that is basically canceled by s_{PR} in its dynamic effects.

Furthermore, Fig. 9 shows that system stability is achieved above a certain pilot gain $K_{P_{crit}}$. It also indicates that there is a significant effect of the prediction time T_{PR} on $K_{P_{crit}}$. This basic result can be confirmed with an analytical solution obtained from evaluating the stability conditions of the closed-loop system. For this evaluation, a pure-gain pilot model is applied ($Y_P = K_P$, without time delay) that is approximately applicable because of $\tau_e \omega \ll 1$ for loop closure with $K_P = K_{P_{crit}}$ where $\omega = \omega_{stab}$ is the stability boundary frequency related to $K_{P_{crit}}$. The following analytical solution holds:

$$K_{P_{crit}} \approx -2/\left(g L_{\delta_a} K_{PR} T_R T_{PR}^3\right) \tag{25}$$

This expression shows that the T_{PR} effect is rather strong (proportional to $1/T_{PR}^3$), yielding a significant and monotonic decrease of $K_{P_{crit}}$ when a larger T_{PR} is selected. Furthermore, there is also an effect of the roll mode time constant according to which $K_{P_{crit}}$ decreases with an increase of T_R.

The stability condition evaluation also yields a solution for the closed-loop frequency at the stability boundary that can be expressed as

$$\omega_{stab} \approx \omega_{PR} \tag{26}$$

A further issue is response quality, flying qualities characteristics, and bandwidth. Here again, the positive response quality characteristics existent with the basic predictor are retained (frequency separation, correspondence between predictor position and vehicle motion, etc.). Furthermore, there is also an improvement. This concerns the mode characteristics determined by the high-frequency roots that are primarily related to roll attitude behavior. As shown in Fig. 9, roll rate feedback introduces an aperiodic motion type for the attitude mode. The aperiodic roll attitude behavior is an aircraft motion response characteristic that is more familiar to the pilot than an oscillatory one that would result in the basic predictor case (Fig. 7). Thus, there is an improvement with respect to the response in roll rate and attitude. System bandwidth shows similar properties as in the basic predictor case according to which the numerator zero frequency ω_{PR} has a significant effect. Some improvement is possible because the stable part of the path mode root locus has frequencies that are larger than ω_{PR}. This follows from the characteristics of the root locus shown in Fig. 9 together with Eq. (26), according to which $\omega > \omega_{PR}$ for $\omega > \omega_{stab}$.

Summing up the foregoing considerations, roll rate feedback primarily concerns the high-frequency region and yields the intended improvements for flight-path control with minimum pilot compensation and for system stability. The positive low-frequency characteristics as they exist with the basic predictor are retained.

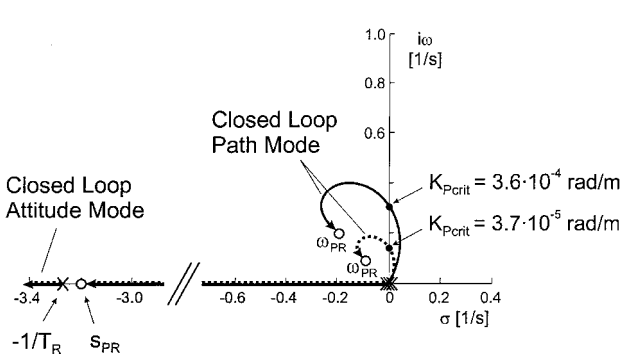

Fig. 9 Root locus of closed-loop system with roll rate feedback [T_R = 0.3 s, pilot model Eq. (4) with τ_e = 0.25 s, K_{PR} = 1.0]: ——, T_{PR} = 5.0 s, and - - - -, T_{PR} = 10.0 s.

Experimental Evaluation

A test program consisting of pilot-in-the-loop simulation experiments was set up to verify the conceptual and theoretical issues. A fixed-base simulator equipped with a perspective flight-path display with a predictor was used. The layout of the predictive flight-path display (with tunnel and predictor as main elements) developed for the experimental program corresponds to the configuration shown in Fig. 1. The nonlinear six-degree-of-freedom aircraft model used in the pilot-in-the-loop simulation experiments can be regarded as representative of small, twin jet engine aircraft. The simulated aircraft has very good dynamics characteristics and flying qualities so that there are no objectionable effects with regard to the flight tasks performed in the simulation experiments related to flight-path prediction. Five pilots with different professional backgrounds (airline pilots, private pilot, student pilot) took part in the simulation experiments where they performed several runs for each flight task. The flight tasks consisted of landing approaches, the ground tracks of which are shown in Fig. 10. Different trajectory profiles were applied to avoid familiarization of the pilots with a fixed trajectory.

A basic issue of the experimental verification is the prediction time T_{PR}, which is a factor of primary concern. This is because it determines the K/s frequency region (together with T_R) and, thus, has a substantial effect on compensatory control characteristics and on related pilot performance. Results of the simulation experiments for the control of the predictor position are presented in Fig. 11 (box plot technique, 95% confidence interval) for different prediction times T_{PR}. As a basic result, the predictor position is effectively controlled by the pilot, with rather small deviations from the command flight-path. Furthermore, the prediction time T_{PR} has a significant effect on the predictor position deviations as controlled by the pilot, with a decrease of the errors when T_{PR} is decreased and vice versa. Results for the corresponding control activity of the pilot are presented in Fig. 12, which shows the aileron deflections for minimizing the deviations of the predictor position. Here again, the effect of T_{PR} is significant, yielding an increase of control activity as T_{PR} is decreased. Comparing the characteristics of control activity and predictor position deviation, it turns out that there is an opposite tendency as regards the effect of the prediction time T_{PR}.

The significant effects of prediction time T_{PR} on predictor position error and control activity can be explained with pilot loop closure behavior. According to Eq. (23), a decrease in prediction time T_{PR} requires an increase in pilot gain for achieving loop closure in the K/s frequency region. As a consequence, the error of the closed-loop system is decreased. The physical reason underlying this phenomenon is that the pilot can suppress excursions more effectively when he can increase his control activity, provided there is an increase of the overall pilot–predictor–aircraft gain.

Further insight into pilot closure characteristics is provided by Fig. 13, which presents frequency response characteristics and pilot–system crossover estimated from the simulation experiments.

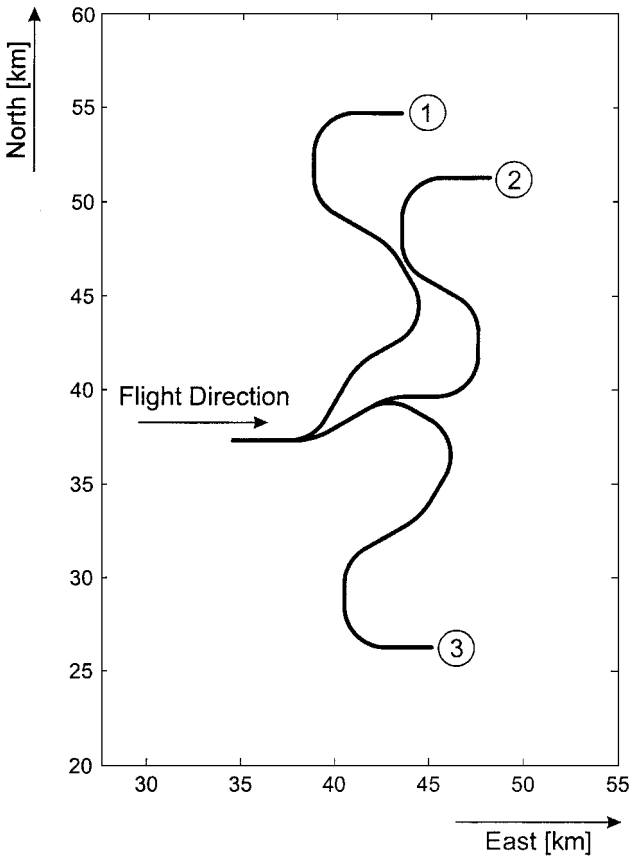

Fig. 10 Approach tracks in simulation experiments.

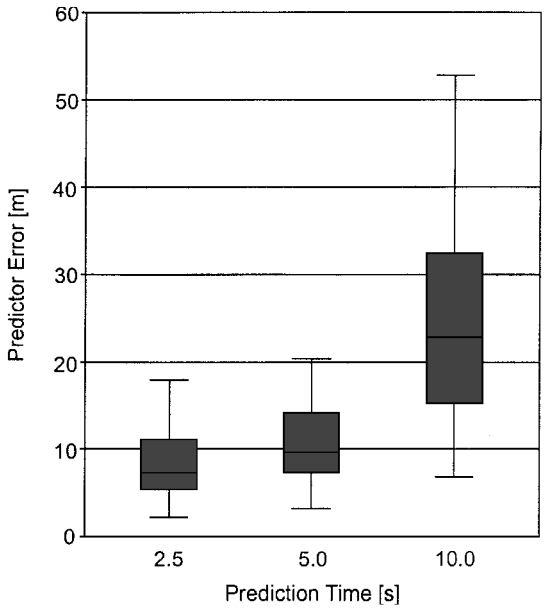

Fig. 11 Deviation of predictor position.

Basically, Fig. 13 shows that pilot–system crossover is in the K/s region and has a large phase margin. Furthermore, the characteristics presented in Fig. 13 can also be used to support the preceding interpretation of the effect of the prediction time T_{PR}. A decrease of T_{PR} would yield a change of ω_{PR} to higher frequencies ($\omega_{PR} = \sqrt{2}/T_{PR}$) so that, in turn, a downward shift of the Bode amplitude of the K/s frequency region results. As a consequence, pilot–system crossover requires an increase in pilot gain (with crossover frequency considered constant).

Another subject of the pilot-in-the-loop simulation program was to show the advantages of roll rate feedback ($K_\phi \dot{\phi}$) by dedicated

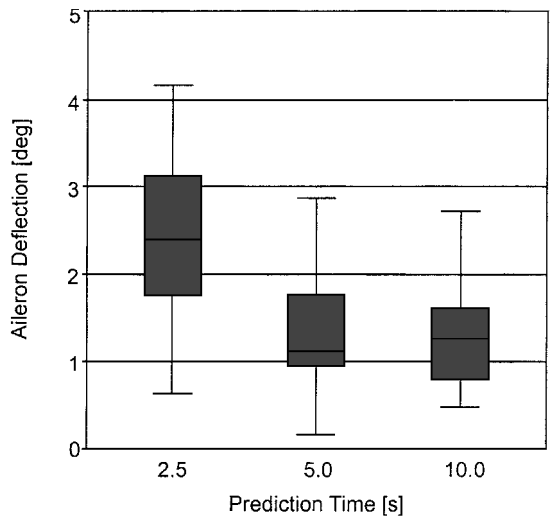

Fig. 12 Pilot control activity.

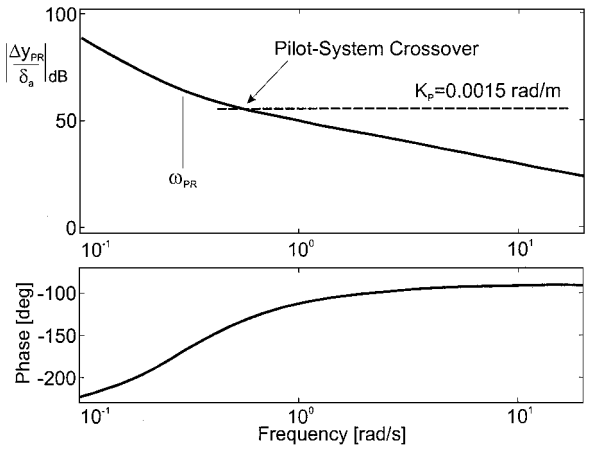

Fig. 13 Frequency response characteristics of predictor–aircraft system and pilot gain from simulation experiments (T_{PR} = 5.0 s, K_{PR} = 1.0).

experiments. Results are presented in Figs. 14 and 15, which show predictor position deviations and related control activity where a predictor with roll rate feedback is considered in comparison to its counterpart without roll rate feedback.

For the predictor without roll rate feedback, there is a significant increase in predictor position deviations when the open-loop roll time constant T_R is increased (Fig. 14). A similar effect holds for the control activity of the pilot (Fig. 15). These results can be explained with pilot loop closure behavior. Basically, an increase of T_R reduces the length of the K/s frequency region so that the K/s^2 frequency region begins at a lower frequency. If this effect is large enough, the pilot may have to develop a lead to achieve a K/s characteristic of the pilot–predictor–aircraft system for crossover. Manual control theory[15,16] shows that, for such a case, the crossover frequency is reduced and the effective time delay of the pilot is increased. As a consequence, a deterioration in performance results. Furthermore, closed-loop stability may be reduced due to phase margin decrease (predictor–aircraft system) and effective time delay increase. In addition, results from pilot questioning after the simulation runs show that the increase of the open-loop roll time constant T_R causes a rating decrement.

Introduction of roll rate feedback yields a substantial improvement. This is illustrated in Figs. 14 and 15, which show that there are several effects. Basically, the predictor position deviations and control activity are significantly reduced when compared to the predictor case without roll rate feedback. Furthermore, the values for the predictor with roll rate feedback in Figs. 14 and 15 stay at a constant level, which indicates that there is no or only a minor influence of the open-loop roll time constant T_R. This even holds for

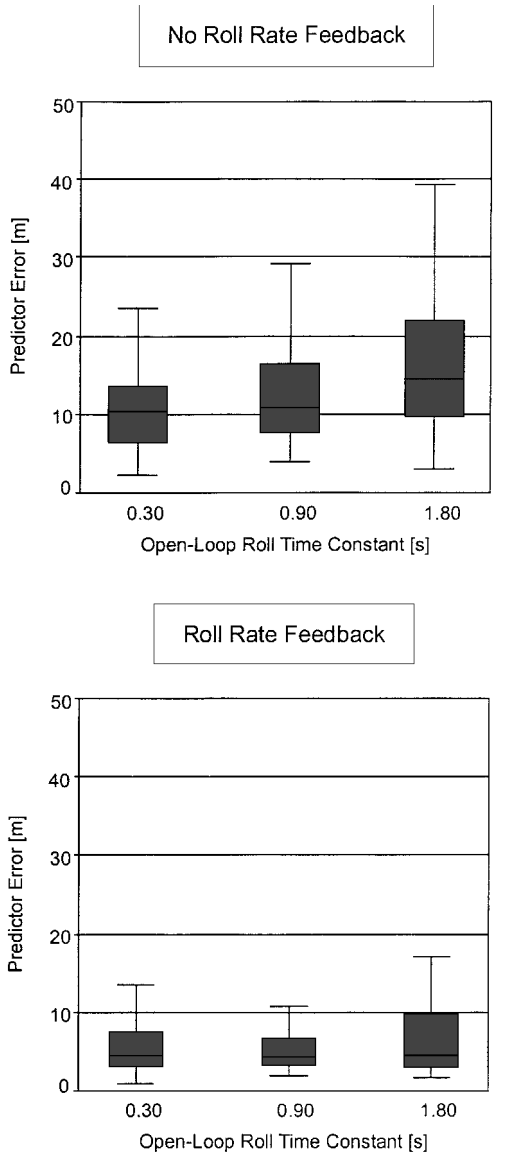

Fig. 14 Effect of roll rate feedback on deviation of predictor position (T_{PR} = 5.0 s).

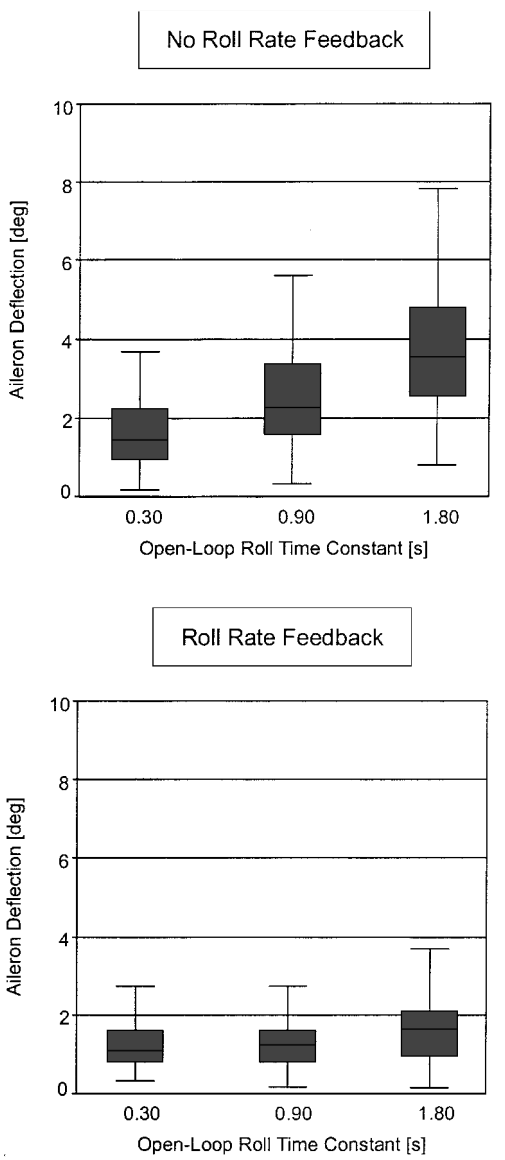

Fig. 15 Effect of roll rate feedback on control activity (T_{PR} = 5.0 s).

the configuration with the largest open-loop roll time constant considered ($T_R = 1.8$ s), which would exceed limits of flying qualities requirements.[17,18] As a result, roll rate feedback yields a compensation of detrimental effects due to large open-loop roll time constants and substantially improves the compensatory control characteristics.

Control of Current State with Predictor

The predictor is originally concerned with the future state of the aircraft at the prediction time ahead, $y(t + T_{PR})$. It is also an efficient means for controlling the current state $y(t)$, which is the ultimate goal of the compensatory control effort of the pilot.

For future state control, the controlled quantity is the position $y(t + T_{PR})$, the deviations of which are to be minimized. With regard to current state control, the controlled quantity is not the position alone but a mixture of quantities including azimuth angle, azimuth rate, and roll rate. Concerning this controlled quantity, the related error denoted by $e_{\text{mix}}(t)$ can be expressed in the following form (according to the pathways of the block diagram shown in Fig. 5):

$$e_{\text{mix}}(t) = \Delta y(t) - y_C^*(t) + K_\chi \Delta\chi(t) + K_{\dot\chi}\Delta\dot\chi(t) + K_\phi\dot\phi(t)$$
$$= \Delta y(t + T_{PR}) = \Delta y_{PR} \tag{27}$$

where

$$K_\chi = VT_{PR}, \qquad K_{\dot\chi} = VT_{PR}^2/2 \tag{28}$$

are gains that, from the standpoint of current state control, have no physical meaning.

Because $e_{\text{mix}} = \Delta y_{PR}$, the results described in the preceding sections about efficient predictor control Δy_{PR} also hold for e_{mix}.

An efficient e_{mix} control also supports an efficient Δy control because of the following reasons:

1) Feedback of χ and $\dot\chi$ with gains K_χ and $K_{\dot\chi}$ were originally introduced for geometry/kinematics reasons to describe the continuation of the flight-path ($K_\chi = VT_{PR}$, $K_{\dot\chi} = VT_{PR}^2/2$). From a control systems standpoint, χ and $\dot\chi$ feedback yields good dynamic characteristics (damping, frequency). This effect of χ and $\dot\chi$ feedback also holds for the control of the current state. Similar arguments with regard to compensatory control apply for $\dot\phi$ feedback.

2) With reference to Eqs. (16) and (20) and to $\Delta y(s) = g\Delta\phi(s)/s^2$, the relation between the current position error $\Delta y(s)$ and the future position error (predictor error) $\Delta y_{PR}(s)$ can be expressed as

$$\frac{\Delta y(s)}{\Delta y_{PR}(s)} = \frac{1}{(T_R s + 1)\left[(s/\omega_{PR})^2 + 2\zeta_{PR}s/\omega_{PR} + 1\right]} \tag{29}$$

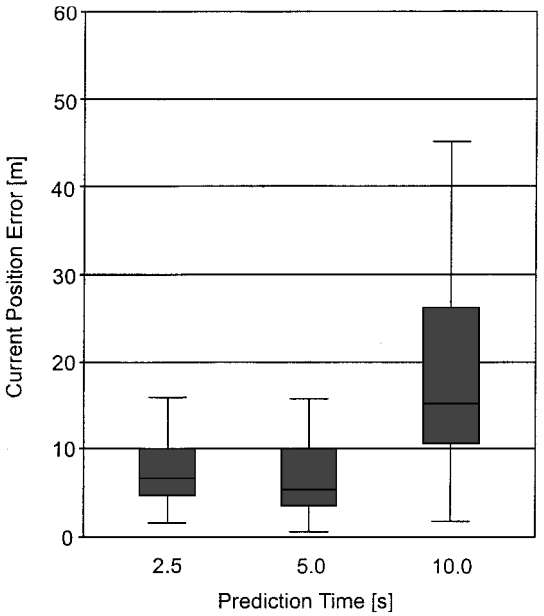

Fig. 16 Deviation of current position.

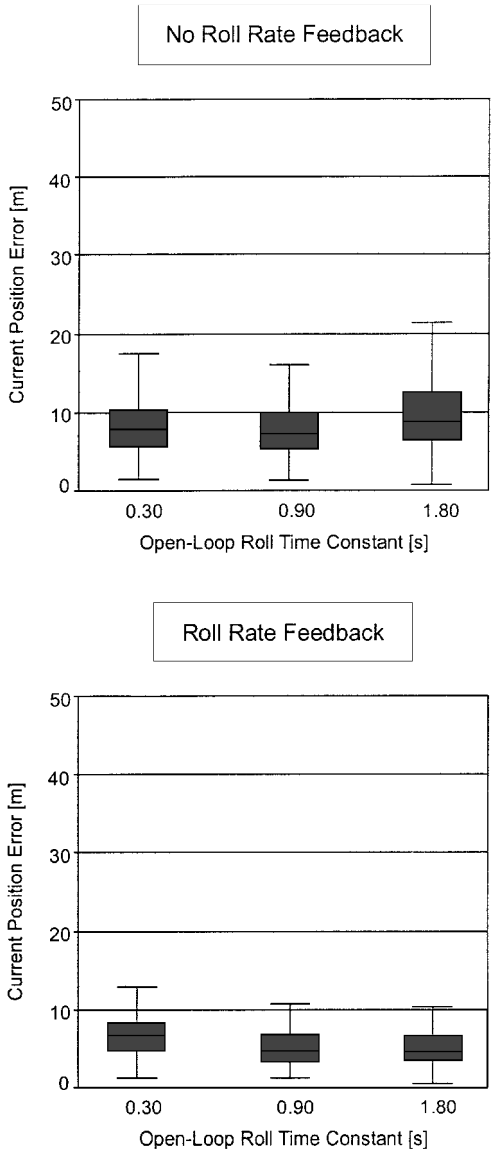

Fig. 17 Effect of roll rate feedback on deviation of current position (T_{PR} = 5.0 s).

According to Eqs. (11) and (19), the damping is $\zeta_{PR} = 1/\sqrt{2}$. For this value, it follows from Eq. (29) for the frequency response characteristics that

$$\left| \frac{\Delta y(s)}{\Delta y_{PR}(s)} \right|_{s=i\omega} \leq 1 \tag{30}$$

As a result, the current position error is basically smaller than the future position error (predictor error). Moreover, Eq. (29) shows that the reduction of Δy relative to Δy_{PR} is very significant for frequencies larger than ω_{PR}. There is a decrease of 40 dB per decade for $\omega_{PR} < \omega < 1/T_R$ and even 60 dB per decade beyond $1/T_R$.

3) Furthermore, both errors approach zero in steady-state reference conditions. This is because, from Eq. (29),

$$\left| \frac{\Delta y(s)}{\Delta y_{PR}(s)} \right|_{s\to 0} = 1 \tag{31}$$

As a result, the current position error becomes zero when the predictor reaches its steady-state reference position, that is, $\Delta y = \Delta y_{PR} = 0$.

The preceding considerations are confirmed with results of the pilot-in-the-loop simulation experiments. Figures 16 and 17 show experimental results for control of the current position Δy (for the same simulator experiments as considered in the preceding section). From the results presented in Figs. 16 and 17, it basically follows that the current state is effectively controlled. Furthermore, comparison with Figs. 11 and 14 shows that the deviations of the current position are even smaller than those of the predictor position. Here again (Fig. 17), roll rate feedback is an efficient means for improving control that shows a particular advantage for large roll time constants.

Conclusions

An aircraft position predictor based on geometry/kinematics relations (model for flight-path continuation) is considered, and a new conceptual predictor extension based on manual control issues is introduced for enhancing the novel guidance and control capabilities possible with perspective flight-path displays. It is shown that the conceptual predictor extension proposed in this paper is an improvement for satisfying pilot-centered requirements for achieving the best performance in compensatory control. This concerns a K/s predictor–aircraft characteristic in an adequately broad region centered around pilot–predictor–aircraft system crossover as well as system stability, response quality, and system bandwidth. It is further shown that the predictor is an efficient means for controlling the flight path not only at the prediction time in the future but also at the current time. Results of pilot-in-the-loop simulation experiments are presented for verification of these issues.

References

[1]Theunissen, E., "Integrated Design of a Man-Machine Interface for 4-D Navigation," Ph.D. Dissertation, Delft Univ. of Technology, Delft, The Netherlands, 1997.

[2]Theunissen, E., and Mulder, M., "Availability and Use of Information in Perspective Flight-path Displays," *Proceedings of the AIAA Flight Simulation Technologies Conference*, AIAA, Washington, DC, 1995, pp. 137–147.

[3]Grunwald, A. J., Robertson, J. B., and Hatfield, J. J., "Experimental Evaluation of a Perspective Tunnel Display for Three-Dimensional Helicopter Approaches," *Journal of Guidance, Control, and Dynamics*, Vol. 4, No. 6, 1981, pp. 623–631.

[4]Grunwald, A. J., "Tunnel Display for Four-Dimensional Fixed-Wing Aircraft Approaches," *Journal of Guidance, Control, and Dynamics*, Vol. 7, No. 3, 1984, pp. 369–377.

[5]Grunwald, A. J., "Predictor Laws for Pictorial Flight Displays," *Journal of Guidance, Control, and Dynamics*, Vol. 8, No. 5, 1985, pp. 545–552.

[6]Grunwald, A. J., "Improved Tunnel Display for Curved Trajectory Following: Control Considerations," *Journal of Guidance, Control, and Dynamics*, Vol. 19, No. 2, 1996, pp. 370–377.

[7]Grunwald, A. J., "Improved Tunnel Display for Curved Trajectory Following: Experimental Evaluation," *Journal of Guidance, Control, and Dynamics*, Vol. 19, No. 2, 1996, pp. 378–384.

[8]Haskell, I. D., and Wickens, C. D., "Two- and Three-Dimensional Displays for Aviation: A Theoretical and Empirical Comparison," *The International Journal of Aviation Psychology*, Vol. 3, No. 2, 1993, pp. 87–109.

[9]Wickens, C. D., Fadden, S., Merwin, D., and Ververs, P. M., "Cognitive Factors in Aviation Display Design," *Proceedings of the 17th AIAA/IEEE/SAE Digital Avionics Systems Conference*, AIAA, Reston, VA, 1998.

[10]Funabiki, K., Muraoka, K., Terui, Y., Harigae, M., and Ono, T., "In-Flight Evaluation of Tunnel-in-the-Sky Display and Curved Approach Pattern," *Proceedings of the AIAA Guidance, Navigation, and Control Conference*, AIAA, Reston, VA, 1999, pp. 108–114.

[11]Sachs, G., and Möller, H., "Synthetic Vision Flight Tests for Precision Approach and Landing," *Proceedings of the AIAA Guidance, Navigation, and Control Conference*, AIAA, Washington, DC, 1995, pp. 1459–1466.

[12]Sachs, G., Dobler, K., and Hermle, P., "Flight Testing Synthetic Vision for Precise Guidance Close to the Ground," *Proceedings of the AIAA Guidance, Navigation, and Control Conference*, AIAA, Reston, VA, 1997, pp. 1210–1219.

[13]Sachs, G., Dobler, K., and Theunissen, E., "Pilot–Vehicle System Control Issues for Predictive Flightpath Displays," *Proceedings of the AIAA Guidance, Navigation, and Control Conference*, AIAA, Reston, VA, 1999, pp. 574–582.

[14]Hess, R. A., and Gorder, P. J., "Design and Evaluation of a Cockpit Display for Hovering Flight," *Journal of Guidance, Control, and Dynamics*, Vol. 13, No. 3, 1990, pp. 450–457.

[15]McRuer, D. T., "Pilot Modeling," AGARD-LS-157, 1988, pp. 2-1–2-30.

[16]Hess, R. A., "Feedback Control Models—Manual Control and Tracking," *Handbook of Human Factors and Ergonomics*, 2nd ed., Wiley, New York, 1997, pp. 1249–1294.

[17]MIL-F-8785C, "Flying Qualities of Piloted Airplanes," 1991.

[18]MIL-STD-1797, "Flying Qualities of Piloted Aircraft," 1990.